Article IV: Metal complexation role of natural organic substrates in reactive mixtures for acid mine drainage *in-situ* treatment

Water Research **(enviat).**

O. Gibert, J. de Pablo, J.L. Cortina, C. Ayora.

METAL COMPLEXATION ROLE OF NATURAL ORGANIC SUBSTRATES ON REACTIVE MIXTURES FOR MITIGATION OF ACID MINE DRAINAGE

Oriol Gibert [1], Joan de Pablo [1,2], José Luis Cortina [1,*], Carlos Ayora [3]

[1] Departament d'Enginyeria Química, ETSEIB, Universitat Politècnica de Catalunya, 08028 Barcelona, Spain.

[2] Departament d'Enginyeria Química, Àrea de Tecnologia Ambiental, Centre Tecnològic de Manresa, 08240 Manresa, Spain.

[3] Institut de Ciències de la Terra Jaume Almera, CSIC, 08028 Barcelona, Spain

Corresponding author phone: 93 4016557; fax: 93 4015814; e-mail: jose.luis.cortina@upc.es

Abstract: The efficiency of the sulphate reducing bacteria-based *in-situ* treatment of acid mine drainages is often limited by the low degradability of the current carbon sources, typically complex plant-derived materials. In such non sulphate-reducing conditions, field and laboratory experiences have shown that mechanisms other than sulphide precipitation should be considered in the metal removal, i.e. metal (oxy)hydroxides precipitation, co-precipitation onto these precipitates, and sorption onto the organic matter.

The focus of the present paper was to present some laboratory data highlighting the Zn and Cu sorption on vegetal compost and to develop a general and simple model for the prediction of their distribution in organic-based passive remediation systems. The model considers two kinds of sorption sites ($\succ SO_2H_2$) and the existence of monodentate and bidentate metal-binding reactions, and it assumes that only free M^{2+} species can sorb onto the compost surface. The acid base properties of the compost were studied by means of potentiometric titrations in order to identify the nature of the involved surface functional groups and their density. The distribution coefficient (K_D) for both Zn and Cu were determined from batch experiments as a function of pH and metal concentration. The model yielded the predominant surface complexes at the experimental conditions, being $\succ SO_2Zn$ for Zn and $\succ SO_2HCu^+$ and $(\succ SO_2H)_2Cu$ for Cu, with $\log K_M$ values of -2.10, 3.36 and 4.65 respectively. The results presented in this study has demonstrated that the proposed model provides a good description of the sorption process of Zn and Cu onto the vegetal compost used in these experiments.

Key words: acid mine drainage, adsorption, natural organic substrate, passive remediation, surface complexation.

INTRODUCTION

The increasing awareness and concern about the environment has motivated in the recent years extensive research into developing new efficient technologies for the acid mine drainage (AMD) remediation. AMD is characterised by high contents of acidity, heavy metals and sulphates, and its potentially damaging impact when it incorporates into the groundwater system has been reported [1].

The recent biological approach in the *in-situ* passive remediation of groundwaters contaminated by AMD is based in the use of sulphate-reducing bacteria (SRB), which are able to reduce sulphate by the oxidation of an organic source, thereby the biogenic sulphide can precipitate most of dissolved heavy metals. However, there are many circumstances that limit the enhancement of the activity of the SRB [2,3], particularly the low degradability of the current carbon sources (typically complex plant-derived materials) used in such treatments. In these non sulphate-reducing conditions, field and laboratory experiences have shown that mechanisms other than sulphide precipitation should be considered in the metal removal, i.e. metal (oxy)hydroxides precipitation, co-precipitation with these precipitates [4], and sorption onto the organic matter [5]. Sorption of heavy metals onto a broad range of low-cost and waste organic materials has successfully been applied to the treatment of industrial effluents and natural waters [6].

This study follows from a previous investigation where vegetal compost was evaluated as a carbon source for SRB in the treatment of AMD. Results revealed that vegetal compost was a poor source of food and energy for bacterial development and that different mechanisms other than SRB activity were responsible for metal removal [7]. Precipitation and co-precipitation mechanisms were discussed, and sorption was anticipated from preliminary tests [8].

The focus of the present paper was to present some laboratory data highlighting the Zn and Cu sorption on vegetal compost, and to develop a general and simple model for the prediction of their distribution in organic-based passive treatments for AMD. In a first step the acid-base properties of the compost will be studied in order to identify the nature of the involved acidic surface functional groups and their density. Then, the distribution coefficient (K_D) for both Zn and Cu will be determined from batch experiments as a function of pH, metal concentration and binding group concentration. The data will be treated numerically to determine the predominant surface complexes at the experimental conditions and their corresponding thermodynamic complexation constants (K).

MATERIALS AND METHODS

Materials. The compost used in this study was prepared by mixing forest woods and sludge and it was provided by a conventional biological treatment plant in Manresa, Catalonia (Spain). An elemental chemical analysis of this compost determined the contents (in wt %) of C (27.2), N (1.3), H (3.4), S (0.5), P (0.9) [9].

Acid-base characterisation of the vegetal compost. Dissolved transition metals can sorb at the interface by exchanging of H^+ at the acidic functional groups [10,11]. Prior to the metal interaction studies, the acid-base properties of the vegetal compost (i.e. the concentration of the total acidic functional groups and their acidity constants) were determined by means of a potentiometric titration. A potentiometric titration consists essentially of the determination of the pH value at which protonation/deprotonation of the acidic functional groups in the solid surface takes place.

Compost was subjected to both acid and basic titrations using an automatic burette system (Micro TT Crison) and a combined glass electrode (Crison 52-02) coupled to a pHmeter (Crison GLP22). In both cases, titrations were conducted following the methodology described elsewhere. A dried sample of compost (1.2 g) was suspended in a reaction vessel containing 20 cm^3 of 0.1 M $NaClO_4$ used as an inert electrolyte to ensure a constant ionic strength. The solution was stirred using a Teflon©-coated magnetic stirring bar, while a small nitrogen overpressure was applied in the vessel. A standarised titrant (0.1 M HCl or 0.1 M NaOH, both containing 0.1 M $NaClO_4$) was added to the vessel and the solution pH was monitored. After each addition, at least 10 min passed to obtain a stable electrode potential. Acid and base titrations of the background electrolyte solution (0.1 M $NaClO_4$) were also conducted as control titrations.

The acid-base characterisation was complemented by Fourier-transform infrared (FTIR) (Perkin Elmer 1600) analysis of compost samples equilibrated with acid (pH=1), neutral (pH=6) and basic (pH=13) aqueous solutions.

Additionally, dissolution of compost with pH was tested and dissolved organic matter (DOM) was quantified by a total organic carbon (TOC) analyser (Shimadzu TOC-5050A).

Metal sorption on vegetal compost. The metal (Zn and Cu) sorption on the compost has been determined from batch experiments as a function of pH, metal concentration and solid:liquid ratios. This study was carried out following standard batch equilibrium experiments. Known volumes (20 cm^3) of prepared metal solutions (concentrations ranging from 4 to 300 mg dm^{-3}, equilibrium pH ranging from 2 to 6.5) were equilibrated with weighted amounts of compost (0.3-1.2 g) in glass tubes using a continuous rotary mixer (50 min^{-1}) at room temperature (22±2ºC) for 15 h. Metal solutions were prepared in a medium containing sulphate (300 mg

dm^{-3}) and carbonate (60 mg dm^{-3}) to better simulate real conditions in the passage of an AMD through a compost/limestone mixture, and 0.1 M $NaClO_4$ to ensure a constant ionic strength. Preliminary tests showed that 15 h was a sufficient time for achieving the metal sorption equilibrium. Thereafter, the equilibrium pH was determined, the remaining aqueous solution was separated by filtration (0.22 μm), and Zn and Cu concentrations were quantified by atomic absorption spectrophotometry (AAS) (Varian Spectra-AA 640) with air-acetylene flame. High Zn concentrations were determined in buffered samples with NH_4^+/NH_3 by a titration procedure with standard EDTA and using Eriochrome Black T as indicator [12].

The metal loading study was complemented by Fourier-transform infrared (FTIR) (Perkin Elmer 1600) analysis of compost samples equilibrated with metal solutions.

RESULTS AND DISCUSSION

Acid-base titration of the compost. A comparison of the acid-base titration data in presence and absence of a compost sample permitted, using a proton balance equation, to compute the net proton/hydroxide uptake Q (mol g^{-1}) by the compost sample from the solution during the acid/base titration, respectively (Figure 1).

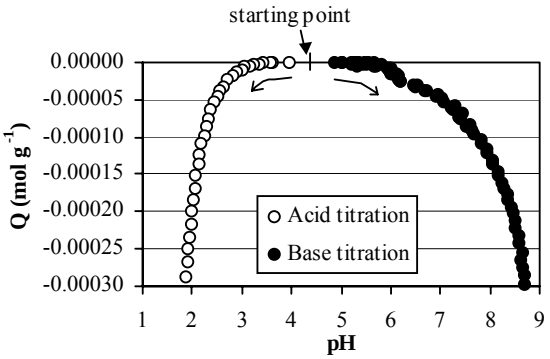

Figure 1. Proton/hydroxide uptake values Q during acid(HCl)/basic(NaOH) titrations respectively (calculated on a dry mass of compost and expressed as negative values).

The acid (HCl) titration curve showed that compost protonation began at pH 3, although the protonation curve did not show any well-defined inflection point. The overlapping of inflection points in titration curves of known polyfunctional ion exchangers is usually observed in real cases [13,14] and attempts to separate them have been reported [14]. At the end of the titration, the concentration of protonated groups was quantified as $3x10^{-4}$ mol g^{-1}. This value is comparable to the maximum sorption capacity (Γ_{max}) of the compost for Zn(II) ($\Gamma_{max}=6x10^{-5}$

mol g^{-1}) and Cu(II) (Γ_{max}=2x10^{-4} mol g^{-1}) determined in a previous study [8].

The basic (NaOH) titration curve showed a discernible weak inflection point at pH around 6.2, with a total OH^- uptake of 4x10^{-5} mol g^{-1}. The final part of the titration curve exhibited a typical vertical drop, suggesting a very weak acid group at pH≈8.7 attributable to phenolic groups [15-17]. This inflection point could not be well-quantified due to a continuous consumption of strong base coupled to a minimum change in pH and to an increase of the colour of the solution (from transparent to a brown colour), indicating compost dissolution. Tube tests on compost dissolution with pH showed that dissolved organic matter (DOM) was below 7 mg dm^{-3} at pH<9, but raised up to 35 mg dm^{-3} at pH 12.7. Similar solid sludge dissolution patterns have been reported, with sharp increases of DOM at pH higher than 8 [18-20]. Because of difficulties in establishing a defined system due to drastic changes of the mass of compost, conventional basic titration technique was not appropriate at alkaline pH. This limitation was not a critical concern in our study because the metal extraction was taking place in the acid to neutral range, and therefore not affected by compost dissolution.

From the acid-base titrations, two kinds of protonation sites can be considered to be present in the vegetal compost. These surface acidic sites can be viewed to belong to a unique functional group with two reactive O^- sites (hereafter referred as $\succ SO_2H_2$)[21] or to two separate functional groups, each with only one reactive O^- site [22]. Among these, and according to De Wit et al. [21] and Gamble et al. [23], the first interpretation was considered in this study in order to simplify the subsequent calculations.

The corresponding equilibrium constants ($K_{H,1}$ and $K_{H,2}$) can be defined by the equations:

$$\succ SO_2H_2 \Leftrightarrow \succ SO_2H^- + H^+ \qquad K_{H,1} = \frac{[\succ SO_2H^-]\{H^+\}}{[\succ SO_2H_2]} \qquad (1)$$

$$\succ SO_2H^- \Leftrightarrow \succ SO_2^{2-} + H^+ \qquad K_{H,2} = \frac{[\succ SO_2^{2-}]\{H^+\}}{[\succ SO_2H^-]} \qquad (2)$$

where $\succ SO_2H_2$ and $\succ SO_2H^-$ are simplified representations of the organic functional group, {} is activity in solution and [ ] denotes the surface concentration. The use of concentrations instead of activities for the surface sites lies in the fact that activities for these species are not directly accessible experimentally, and [ ]= {} will be considered.

The total acidic sites concentration (T_S) can be defined as the sum of the protonated and deprotonated sites (T_S= [$\succ SO_2H_2$]+[$\succ SO_2H^-$]+[$\succ SO_2^{2-}$] (mol g^{-1})).

Determination of the acidity constants. The acidic surface sites undergo protonation/dissociation equilibria. The extent to which they protonate/deprotonate is controlled by the acidity constant (K_H) and pH, which experimentally can be related by the Modified Henderson-Hasselbach equation [24]:

$$pH = pK_H + n\log\frac{\alpha}{1-\alpha} \qquad (3)$$

where α is the degree of dissociation of the acidic functional group and pK_H and n are empirical constants. Figure 2 shows the variation of the pH versus $\log(\alpha/(1-\alpha))$ for both the acid (HCl) and basic (NaOH) titration curves of the vegetal compost.

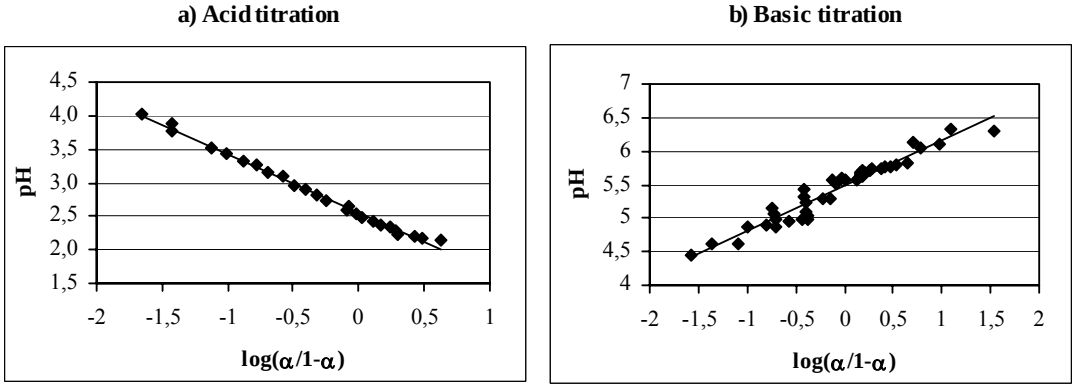

Figure 2. Variation of the pH versus $\log(\alpha/(1-\alpha))$ for both a) acid (HCl) and b) basic (NaOH) titration curves of the vegetal compost. In the basic titration, points at pH>6.5 were omitted due to compost dissolution.

According eq (3), pK_Hs can be derived from Figure 2 as the intercept of the pH vs $\log(\alpha/(1-\alpha))$, leading to a log $K_{H,1}$ of -2.5 (±0.1) and log $K_{H,2}$ of -5.5 (±0.2).

Functional groups identification. The (ortho isomer) and salicylic acids (Figure 3) have been widely used as analogues to humic substances to simulate the sorptive properties of natural organic matter [21,23]. The pKa_1 of o-phtalic acid is 2.9, similar to the pKa_1 of salicylic acid. The second carboxylic group in o-phtalic acid has a pKa_2 of 5.5 indicating a higher proton affinity, while the pKa_2 of salicylic acid, arising from dissociation of the proton, is 13.4.

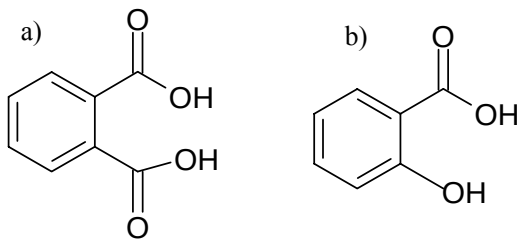

Figure 3. Structure of (a) o-phtalic acid and b) salicylic acid as models for natural organic matter.

The $pK_{H,1}$ (2.9) and $pK_{H,2}$ (5.5) corresponding to the compost acidic sites can thus be ascribed to the protonation of the functional groups of o-phtalic acid and salicylic acid-like structures. pK_H of 5,5 could also be ascribed to phosphonate groups [20], but this attribution was ruled out in our study owing to the low contents of phosphor in the compost and the lack of phosphonates groups in the FTIR spectra (see later Figure 5).

These findings are in agreement with studies reporting carboxylic and phenolic groups as the major acidic functional groups present in natural organic matter [10,11,13,16,25]. These studies have fitted experimental data to a range of acidities for more acid (carboxylic) and less acid (phenolic) groups of humic and fulvic acids [15-17] and have concluded that experimental data can be in most cases adequately modelled using one or two types of acidic sites [11,18,23]. Table 1 compiles published results in acid-base characterisation of several carbonaceous materials, poly-functional ion exchangers and biosorbents. It also includes pK_Hs values for vegetal compost obtained in this study from acid-base titrations.

Material	Group	T_S (mol g^{-1})	pK_H	Reference
Activated Carbon	n.i.	n.a.	2.3	[15]
NUCHAR SA	n.i.	n.a.	5.7	
Activated Carbon	Phenol	n.a.	8.6	[15]
F400	Phenol	n.a.	12.2	
Activated Carbon	Phenol	n.a.	9.97	[16]
(apricot stones)				
Activated Carbon	Pyrone type	0.88	1.84	[16]
(from apricot stones,	n.a.	0.15	4.77	
after air oxidation)	n.a.	0.67	6.90	
	Phenol	0.95	9.72	
	Phenol	1.02	11.46	
Activated Carbon	Pyrone type	0.65	2.0	[16]
(from apricot stones,	n.a.	0.45	4.14	
after acid oxidation)	n.a.	0.84	6.51	
	Phenol	1.48	10.05	
Phosphorous	Polyphosphates/	0.69	2.45	[16]
containing carbon	phosphonic-phosphonous	0.22	4.57	
	acid/ phosphines	0.89	6.79	
	n.a.	0.80	9.90	
Algal biosorbent (BK)	Carboxyl	4.99	3.19	[16]
Durvillea Potatorun	n.i.	2.15	7.29	
	n.a.	6.05	11.81	
Algal biosorbent (LH)	Carboxyl	2.08	4.00	[16]
Laminaria Hyperborea	n.i.	2.14	7.17	
	n.a.	3.57	11.81	
Polyacrylic ion		0.16	2.24	[16]
exchange resin	Carboxyl	1.15	4.08	
		3.41	5.63	
Brawn seaweed	Carboxyl	2.57	3.70	[20]
Sargassum polycystum	Phosphonate	0.45	5.41	
	Amine	0.65	8.77	
DOM from	Carboxyl	n.a.	5.3	[18]
sludge	Amino	n.a.	9.5	
Seafood processing	Carboxylic	1.71	5.80	[17]
waste sludge	Hydroxil	n.a.	9.55	
	Amine	n.a.		
Dealginated Seaweed	Carboxyl	n.a.	3,63	[26]
Waste	Thiol/Amine	n.a.	9,09	
Vegetal compost	Carboxylic	0.3	2.50	This study
	Carboxylic	0.04	5.50	

n.i.: non identified, n.a.: not available data.

Table 1. Reported results in acid-base characterisation of several carbonaceous materials, poly-functional ion exchangers and biosorbents. T_S accounts for the total acidic groups concentration (in mol g^{-1} solid).

FTIR analysis. Figure 4 compares the general features of the FTIR spectra of compost samples equilibrated with acid (pH=1), neutral (pH=6) and basic (pH=13) in order to identify the nature of the acid-base groups present in the compost.

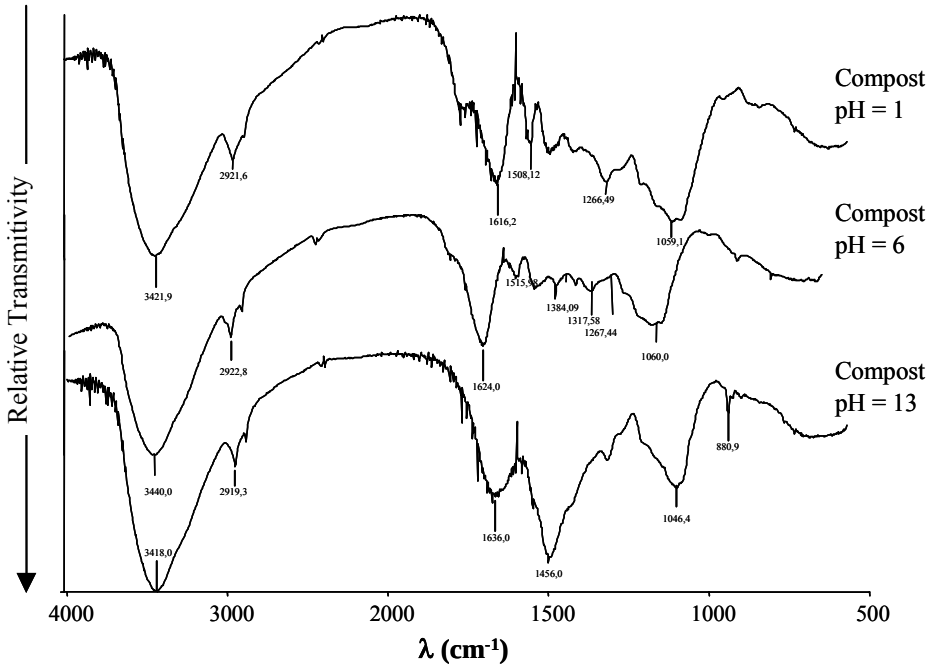

Figure 4. FTIR spectra of organic matter sample equilibrated at different pH values (6, 1 and 13) using KBr discs.

The spectrum of compost equilibrated at pH 6 showed a broad band at 3440 cm^{-1} (ascribed to the stretching mode of OH, CH, NH) [27-29], and two smaller bands at 1623 cm^{-1} (carboxylate $RCOO^-$) [18,27,29], with a slight shoulder at around 1700 cm^{-1} (carboxylic RCOOH) [27,30,31], and at 1060 cm^{-1} (carbohydrate or polysaccharide) [22,27]. Smaller peaks at 2922 cm^{-1} (stretching modes of the aromatic and aliphatic C-H groups), 1515 cm^{-1} (C=C ring stretching), 1384 cm^{-1} (COO, CH_3 stretching or OH stretching), 1267 cm^{-1} (aromatic C, C-O stretching) [22,27,32] are observed.

Equilibration of compost at acid (pH=1) and basic (pH=13) media induced the following perturbations: (1) the band at 3440 cm^{-1} increased in intensity and shifted to lower frequencies in both cases, indicating protonation and deprotonation of the R-OH group to $R\text{-}OH_2^+$ and $R\text{-}O^-$, respectively; (2) the shoulder at the 1730-1750 cm^{-1} region increased in the acidified sample, while disappeared in the basified sample, indicating the presence of carboxylate groups, which are protonated/deprotonated depending on pH. The trend of the variation of carboxylate/carboxylic peaks with pH in FTIR spectra is reported in the literature [25]; (3) the

band at 1624 cm^{-1} shifts to lower frequencies in the acidified sample but to higher frequencies in the basified sample. This shift indicates perturbations of carboxylate groups with pH; (4) a strong broad peak appears at 1456 cm^{-1} in the basified sample, which is assigned to the stretching of C=O in inorganic carbonates CO_3^{2-} [31]. The apparition of the peak at 880.4 cm^{-1}, ascribed to the C-O stretching of the CO_3^{2-}, supports this hypothesis [31]. The presence of inorganic CO_3^{2-} in the basified sample is likely due to the degradation of the organic matter, which is induced by high pH values, and subsequent carbonate precipitation.

Metal sorption on vegetal compost. The extent of the metal sorption has been described in basis of the distribution coefficient ($K_{D,M}$), which can be defined as:

$$K_D = \frac{[M]_s}{[M]_{aq}} = \frac{([M]_0 - [M]_{aq})(V/m_s)}{[M]_{aq}} \qquad (4)$$

where $[M]_s$ and $[M]_{aq}$ denote the total metal concentration in the solid (in mol kg^{-1}) and the aqueous phases (mol dm^{-3}) once the sorption equilibrium has been achieved, $[M]_0$ is the initial total concentration of metal in the aqueous phase, V denotes the volume of the aqueous phase (dm^3), and m_s is the weight of vegetal compost based on a dried mass (kg). It is worth noting that the appropriate use of K_D is restricted only as long as a linear relationship between the concentrations in the solid and aqueous phases is valid, i.e. before saturation of sorption capacity, and an equilibrium situation prevails.

In this section, the dependence of K_D with pH and $[M]_{aq}$ for a given adsorbent/adsorbate (V/m_s) ratio has been investigated.

Effect of pH on K_D: Figure 5 shows the $\log K_D$ dependence with equilibrium pH for both Zn and Cu. Experiments were conducted at an equal compost dose (0.3 g solid per 20 cm^3 liquid) and initial $[M]_0$ (20 mg dm^3), whereas equilibrium pH were differently adjusted by the addition of HCl/NaOH solutions. Adsorption on the compost increased by increasing pH, with a linear dependence until a plateau is reached from pH 6 for Zn(II) and from pH 4 for Cu(II). This trend indicates a strong competition between protons and metal ions for the available binding sites, as widely reported in the literature [10,11,17,22]. The fitting curves in Figure 5 have been drawn taking into account the proposed model developed in the subsequent section.

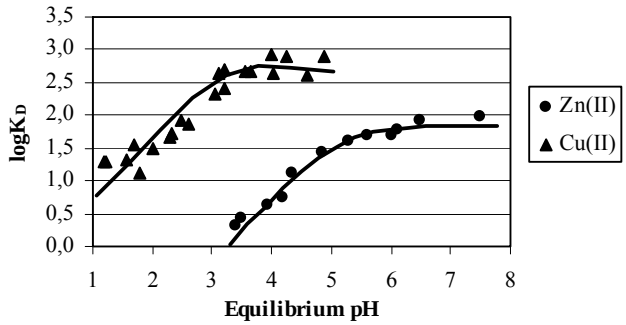

Figure 5. Variation of $\log K_D$ as a function of equilibrium pH at equal compost dose (0.3 g solid per 20 cm^3 liquid) and initial $[M]_0$ (20 mg dm^{-3}). Points are experimental data and curves are calculated with the proposed model.

Effect of $[M]_{aq}$ on K_D: Figure 6 plots experimental $\log K_D$ values versus equilibrium $[M]_{aq}$. Experiments were conducted at equal compost dose (0.3 g solid per 20 cm^3 liquid) and equilibrium pH (subsequently readjusted to 6.5 for Zn and 5.5 for Cu). Adsorption isotherms of Zn and Cu onto the vegetal compost obtained in a previous study [8] showed a linear range within an equilibrium aqueous concentration up to 40 mg dm^{-3} ($10^{-3.2}$ M) for Zn and 110 mg dm^{-3} ($10^{-2.7}$ M) for Cu. Figure 7 shows in fact that when Zn and Cu concentrations are unequivocally within the linear region of the adsorption isotherm, experimental $\log K_D$ has a constant value (ca. 1.6 for Zn and ca. 1.8 for Cu). At higher metal concentration, a slight deviation occurs due to saturation of the compost. The fitting curves in Figure 7 have been drawn taking into account the proposed model developed below.

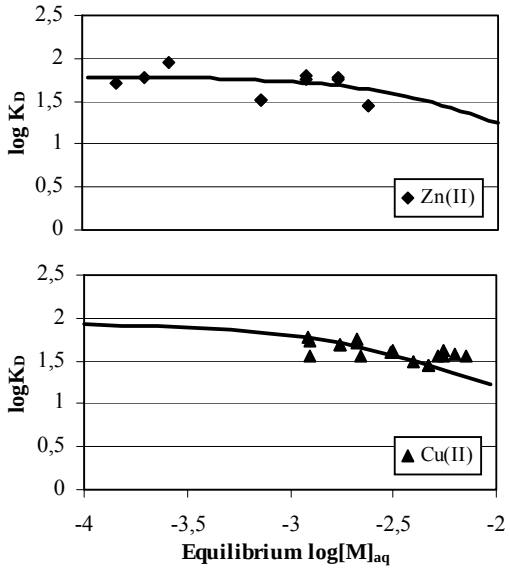

Figure 6. Variation of $\log K_D$ as a function of equilibrium $\log[M]_{aq}$ at equal compost dose (0.3 g solid per 20 cm^3 liquid) and equilibrium pH (subsequently readjusted to 6.5 for Zn and 5.5 for Cu). Points are experimental data and curves are calculated with the proposed model.

Model development. The model development requires a priori the choice of the reactive species and reactions to be included in the model. The species that will be taken into consideration are those characterising the experimental studies conducted in this work, i.e. protons, metals -we will focus on Zn and Cu-, sulphates and carbonates, which are present in the aqueous phase, and compost, which constitutes the solid phase. The set of reactions to be taken into account include the metal-compost complexation, the aqueous ligand-metal complexation, and the metal precipitation.

The metal complexation mechanisms proposed in this study are described by means of the following monodentate and bidentate reactions:

Monodentate reactions:

$$\succ SO_2H^- + M^{2+} \Leftrightarrow \succ SO_2HM^+ \qquad K_{M,1} = \frac{[\succ SO_2HM^+]}{[\succ SO_2H^-]\{M^{2+}\}} \qquad (5)$$

$$\succ SO_2H^- + M^{2+} \Leftrightarrow \succ SO_2M + H^+ \qquad K_{M,2} = \frac{[\succ SO_2M]\{H^+\}}{[\succ SO_2H^-]\{M^{2+}\}} \qquad (6)$$

Bidentate reactions:

$$2(\succ SO_2H^-) + M^{2+} \Leftrightarrow (\succ SO_2H)_2M \qquad K_{M,3} = \frac{\left[(\succ SO_2H)_2\ M\right]}{\left[\succ SO_2H^-\right]^2 \{M^{2+}\}} \qquad (7)$$

$$2(\succ SO_2H^-) + M^{2+} \Leftrightarrow (\succ SO_2)_2M^{2-} + 2H^+ \qquad K_{M,4} = \frac{\left[(\succ SO_2)_2\ M^{2-}\right]\{H^+\}^2}{\left[\succ SO_2H^-\right]^2 \{M^{2+}\}} \qquad (8)$$

where M represents Zn or Cu, $K_{M,i}$ represent the stoichiometric equilibrium constants and, analogously to eqs 1 and 2, {} and [ ] represent activities and concentrations, respectively. Surface complexation constants describe the extent to which the $\succ$SOH sites bind cations. The greater the value of K_M the more preferred is the metal bound to the sorbent. From the acid-base characterisation of the compost, carboxylate groups may be ascribed to be responsible for metal sorption in circumneutral and low pH.

Cu(II) and Zn(II) were not the only ones present in the solution, Na^+ were added in the system as Na_2SO_4 and $NaHCO_3$ when providing a sulphate and carbonate rich medium similar to that encountered in an AMD-compost/limestone system. However, the inability of Na^+ to compete for sorption sites in natural organic matters has been reported [32], and it can be assumed that no cations other than M^{2+} and H^+ can occupy the sorption sites.

The aqueous ligand-metal complexation and metal precipitation occurrence in our systems was studied using the Medusa equilibrium code and Hydra thermodynamic database [33]. At the pH of this work, the predominant dissolved species for both Zn and Cu were found to be $M^{2+}_{(aq)}$ and $M\text{-}SO_{4(aq)}$. The contribution of $M\text{-}CO_3$ and M-OH complexes was found to be less than 5% and were neglected in further calculations. Metals might also react with dissolved organic matter (DOM) to form M-DOM complexes. However, DOM content was always quantified below 7 mg dm^{-3}, which led us to consider the M-DOM complexation as a minor process and would not play an important role in the extraction mechanism. Significant DOM contents were only found at pHs above than 9, which were far higher than the pH of this study. Concerning the metal precipitation by hydrolysis, the thermodynamic calculations showed that it occurs at pH>6.5 for Cu^{2+} and pH>8 for Zn^{2+}, higher than the experimental pH in our experiments (between 3 to 6 for Zn^{2+} and between 1 to 5 for Cu^{2+}).

Taking into account the proposed model, the solid phase quantity (numerator) in eq 4 can be expanded in terms of binding equilibria (eqs 5-8), while the liquid phase quantity (denominator) can be expanded in terms of the predominant dissolved species:

$$[M]_s = [\succ SO_2HM^+]_s + [\succ SO_2M]_s + [(\succ SO_2H)_2M]_s + [(\succ SO_2)_2M^{2-}]_s$$

$$=[M^{2+}]_s[\succ SO_2H^-]\left(K_{M,1} + \frac{K_{M,2}}{[H^+]} + K_{M,3}[\succ SO_2H^-] + \frac{K_{M,4}[\succ SO_2H^-]}{[H^+]^2} \right) \quad (9)$$

$$[M]_{aq} \approx [M^{2+}] + [MSO_4]_{aq} = [M^{2+}]_{aq}(1+\beta_{M,S}[SO_4^{2-}]) \quad (10)$$

where $\beta_{M,S}$ is the aqueous complexation constant for $MSO_{4(aq)}$ $\beta_{M,S}=[MSO_4]/[M^{2+}][SO_4^{2-}]$.

Introducing eqs 9 and 10 into eq 4 yields:

$$K_D = \frac{[\succ SO_2H^-]\left(K_{M,1} + \frac{K_{M,2}}{[H^+]} + K_{M,3}[\succ SO_2H^-] + \frac{K_{M,4}[SO_2H^-]}{[H^+]^2} \right)}{1+\beta_{M,s}[SO_4^{2-}]} \frac{V}{m_s} \quad (11)$$

According to eq 11, the distribution coefficient K_D for a given adsorbent/adsorbate (V/m_s) ratio depends ultimately on pH. It should be noted that eq 11 remains valid as long as (1) total metal concentration is small in relation to the concentration of surface groups, i.e. there is no saturation of adsorption sites and sorption is not influenced by the neighbour occupied sites and the concentration of the sorbed species can be equated to thermodynamic activity; (2) the solution is diluted enough to assume that molarity is equal to molality; (3) metal complexation with OH^- and CO_3^{2-} can be neglected; (4) $[SO_4^{2-}]$ remains virtually unchanged, i.e. it is present at higher concentrations than those encountered with metals; (5) the ionic strength and the thermodynamic activity coefficients for aqueous species remain practically constant.

Experimental K_D data obtained at different pH and metal concentrations (Fig 5 and 6) were evaluated using the computer LETAGROP-DISTR program [34]. For a given model, this program searches the best set of equilibrium constants K_i that minimises the error squares sum defined as:

$$U = \sum (\log K_{D,exp} - \log K_{D,calc})^2 \qquad (12)$$

where $K_{D,exp}$ is the distribution ratio of metal determined experimentally and $K_{D,cal}$ is the value calculated by the program solving the mass balance equation for $[M]_s$, $[M]_{aq}$ and sulphate, assuming a particular set of species and constants.

This program also calculates the standard deviation $\sigma(\log K_D)$ defined by:

$$\sigma(\log K_D) = (U/N_P)^{1/2} \qquad (13)$$

where N_p is the difference between total number of experimental points and the total number of equilibrium constants calculated.

Several models considering different complexation reactions (combinations of eq 5-8) for both Zn and Cu were tested by determining the equilibrium constants in order to fit the experimental data. The results obtained in these calculations are listed in Table 2.

	Model #	Species	$\log K_i$	U	$\sigma(\log K)$
Zn	1	$\succ SO_2Zn$	-2.10±0.09	0.48	0.13
	2	$\succ SO_2HZn$	3.61±0.32	22.8	1.03
	3	$\succ (SO_2H)_2Zn$	5.55±0.43	69.1	1.60
	4	$\succ (SO_2)_2Zn^{2-}$	-5.97±0.23	5.51	0.45
	5	$\succ SO_2Zn$	-2.10±0.09	0.48	0.13
		$\succ SO_2HZn$	rejected*		
	6	$\succ SO_2Zn$	-2.10±0.09	0.48	0.13
		$\succ (SO_2H)_2Zn$	rejected*		
	7	$\succ SO_2Zn$	-2.10±0.09	0.48	0.13
		$\succ (SO_2)_2Zn^{2-}$	rejected*		
Cu	1	$\succ SO_2Cu$	-2.67±0.15	6.20	0.13
	2	$\succ SO_2HCu^{+}$	3.79±0.23	3.70	1.03
	3	$\succ (SO_2H)_2Cu$	4.58±0.20	5.51	1.60
	4	$\succ (SO_2)_2Cu^{2-}$	-2.87±0.22	7.80	0.45
	5	$\succ SO_2HCu^{+}$	3.36±0.25	2.80	0.21
		$\succ (SO_2H)_2Cu$	4.65±0.31		
	6	$\succ SO_2HCu^{+}$	3.76±0.21	3.90	0.31
		$\succ (SO_2)_2Cu^{2-}$	rejected*		
	7	$\succ SO_2HCu^{+}$	3.76±0.32	5.80	0.30
		$\succ SO_2Cu$	0.36±0.14		
	8	$\succ SO_2HCu^{+}$	3.60±0.15	3.90	0.31
		$\succ (SO_2)_2Cu^{2-}$	rejected*		
	9	$\succ (SO_2H)_2Cu$	4.55±0.21	5.51	1.60
		$\succ (SO_2)_2Cu^{2-}$	rejected*		
	10	$\succ SO_2Cu$	-2.01±0.15	4.80	0.34
		$\succ (SO_2H)_2Cu$	4.87±0.21		

*rejected: negligible value

Table 2. Description on the calculation details for the set of models evaluated for Zn and Cu(II) sorption onto the vegetal compost used in this study at a ionic strength of 0.1.

The best-fitting models were set #1 for Zn and set #5 for Cu. Their corresponding surface complexes were $\succ SO_2Zn$ for Zn and $\succ SO_2HCu^+$ and $(\succ SO_2H)_2Cu$ for Cu, with $\log K_M$ values of –2.10, 3.36 and 4.65 respectively. The greater values of K_{Cu} than K_{Zn} deal with the sorption preference of vegetal compost for Cu over Zn [8] as found with other organic matters as biosorbents [5,15,19]. The obtained $K_{M,i}$ values were also used to draw the fitting curves in Figures 5-6.

Finally, Figure 7 shows the distribution diagram for Zn(II) and Cu(II) species in the aqueous and solid phases as a function of pH and using the $K_{M,i}$ obtained in this study.

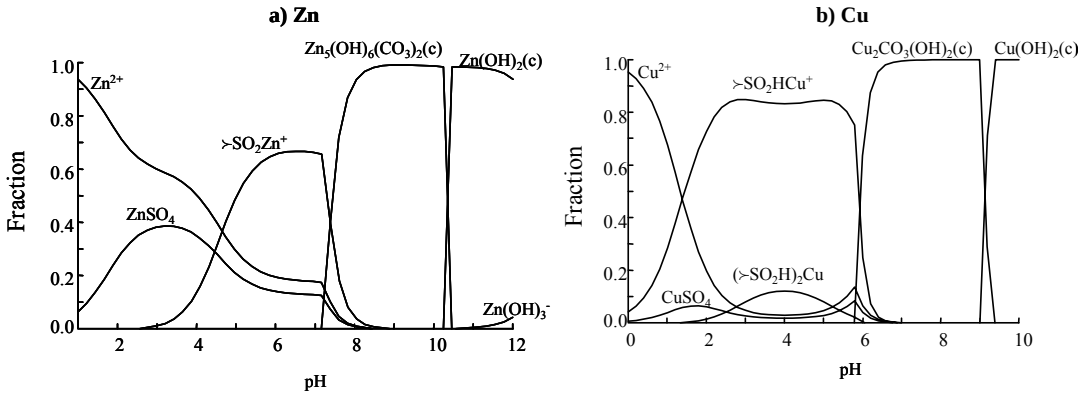

Figure 7. Species distribution diagram as a function of pH for the system a) compost-Zn^{2+}-CO_3^{2-}-SO_4^{2-}-H_2O and b) compost-Cu^{2+}-CO_3^{2-}-SO_4^{2-}-H_2O, with metal concentration of 20 mg dm^{-3} in a sulphate (300 mg dm^{-3}) and carbonate (60 mg dm^{-3}) medium (from Medusa equilibrium calculation codes and Hydra thermodynamic database)[33].

Validation of the model. The model described was applied to predict the results of independent experiments of sorption for different compost/liquid ratios. Experiments were conducted at equal initial metal concentration ($[M]_0$=20 mg dm^3) and equilibrium pH (6.5 for Zn and 5.5 for Cu). Metal solutions were prepared in a medium containing sulphate (300 mg dm^{-3}) and carbonate (60 mg dm^{-3}) and 0.1 M $NaClO_4$. The compost doses ranged between 0.3 and 1.2 g in 20 cm^3 of aqueous phase.

Metal sorption results were represented in terms of extraction percentages (E(%)) versus $[\succ SO_2H^-]$. E(%) is related to K_D according the following equation:

$$E(\%) = \frac{K_{D,M}}{1 + K_{D,M}\left(V/m_s\right)} \qquad (14)$$

The advantage of representing the metal sorption in terms of E(%) instead of K_D lies in the fact that E(%) values obtained at different V/m_s ratios can be fitted with the same modelling curve.

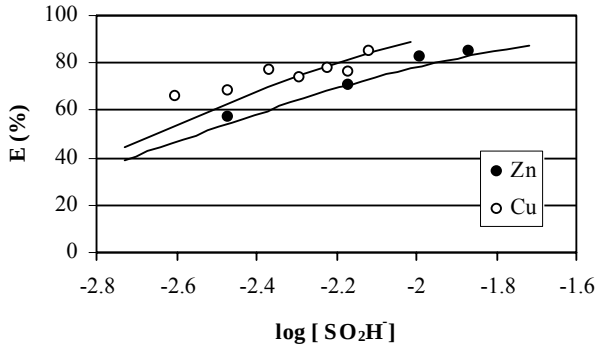

Figure 8. Extraction percentage as a function of [$\succ SO_2H^-$] (compost dose 0.3-1.2 g, aqueous phase volume 20 cm^3) at equal initial $[M]_0$ (20 mg dm^3) and equilibrium pH (subsequently readjusted to 6.5 for Zn and 5.5 for Cu). Points are experimental data. The fitting curves have been generated taking into account the proposed model

As expected, the extraction percentage increases with increasing the compost dose (Fig 8). The fitting between the predicted and the experimental values are very good for Zn and reasonable for Cu.

FTIR analysis of compost-Zn(II) and Cu(II) interaction. A comparison of spectral assignments of the main bands for both spectra of Zn(II)- and Cu(II)- loaded compost with those for the raw compost showed that the metal load shifted the 3440 cm^{-1} band to lower frequencies for both metals and the 1624 cm^{-1} band in Cu-loaded compost, while the 1267 cm^{-1} band slightly increased to higher frequencies. These perturbations suggested the involvement of the carboxyl and phenol groups in the metal biosorption. The involvement of carboxyl groups is in agreement with the previous discussion. The phenolic group (protonable at pH>8 as found in the basic potentiometric titration) in natural organic structures are reported to be often located next to stronger, directly titratable acid groups (Figure 3b) and, although they are weak acid groups, in the presence of M^{2+} can release H^+ to provide a favourable bidentate ligand geometry to form stable complexes with M^{2+} [13,23]. Examples of this proton-release in the presence of heavy metal ions are reported in the literature [13].

ACKNOWLEDGEMENTS

We gratefully acknowledge to T. Bönnemar and A. Vázquez for help assistance in laboratory, to Dr. Lurdes Franco for FTIR analysis and to Dr. J. Bou (Polymer Chemistry Laborataory) for helping in FTIR interpretation. This work was funded by the EU PIRAMID project (EVK1-1999-00061P) and by the Spanish MCYT programmes (REN-2002-04055-CO2 and REN2003-09590-CO4).

LITERATURE CITED

(1) Younger, P.L.; Banwart, S.A.; Hedin, R.S. *Minewater: Hydrology Pollution and Remediation*; Kluwer Academic Publishers: Dordrecht, 2002.

(2) Scherer, M. M.; Richter, S.; Valentine, R.L.; Alvarez, P.J.J. *Crit. Rev. Microbiol.* **2000**, 26, 221-264.

(3) Gibert, O.; de Pablo, J.; Cortina, J.L.; Ayora, C. *Rev Environ. Sci. Technol.* **2002**, 1, 327-333.

(4) McGregor, R.G.; Blowes, D.W.; Jambor, J.L.; Robertson, W.D. *Environ. Geol.* **1998**, 36, 305-319.

(5) Machemer, S.D.; Wildeman, T.R. *J. Contam. Hydrol*. **1992**, 9, 115-131.

(6) Lister, S.K.; Line, M.A. *Biores. Technol*. **2001**, 79, 35-39.

(7) Gibert, O.; de Pablo, J.; Cortina, J.L.; Ayora, C. *J. Chem. Technol. Biotechnol.* **2003**, 78, 489-496.

(8) Gibert, O.; de Pablo, J.; Cortina, J.L.; Ayora, C. *Appl.Geochem,* submitted for publication.

(9) Gibert, O.; de Pablo, J.; Cortina, J.L.; Ayora, C. *Water Res.* submitted for publication.

(10) Boily, J.F.; Fein, J.B. *Chem. Geol.* **2000**, 168, 239-253.

(11) Čežíková, J; Kozler, J.; Madronová, L.; Novák, J.; Janoš, P. *React. Funct. Polym.* **2001**, 47, 111-118.

(12) Vogel, A.I. *Textbook of Quantitative Inorganic Analysis*; Longman: London, 1978.

(13) Ephraim, J.M.; Allard, B. In *Ion Exchange and Solvent Extraction, volume 11*; Marinsky, J.A., Marcus, Y., Eds; Marcel Dekker: New York, USA, 1993; pp 335-362.

(14) Soldatov, V.S. In *Proceedings of IEX2000, Ion Exchange at the Millennium*, Greig, J.A. Ed; Imperial College Press, London, UK, 2000; pp 193-200.

(15) Huang, C.P.; Hsieh, Y.S.; Park, S.W.; Corapcioglu, M.O.; Bowers, A.R.; Elliott, H.A. in *Metals Speciation, Separation and Recovery*, Patterson, J.W., Passino, R., Eds; Lewis Publishers: Michigan, USA, 1990; pp 437-465.

(16) Malik, D.J.; Strelko, V.; Streat, M.; Puziy, A.M. In *Proceedings of IEX2000, Ion Exchange at the Millennium*, Greig, J.A. Ed; Imperial College Press, London, UK, 2000; pp 369-376.

(17) Lee, S.M.; Davis, A.P. *Water Res*. **2001**, 35, 534-540.

(18) Wang, J.; Huang, C.P.; Allen, H.E.; Takiyama, L.R.; Poesponegoro, I.; Poesponegoro, H.; Pirestani, D. *Water Environ. Res.* **1998**, 70, 1041-1048.

(19) Wang, J.; Huang, C.P.; Allen, H.E.; Poesponegoro, I.; Poesponegoro, H.; Takiyama, L.R.; *Water Environ. Res.* **1999**, 71, 139-147.

(20) Yun, Y.S.; Volesky, B. *Environ. Sci. Technol.* **2003**, 37, 3601-3608.

(21) De Wit, J.C.M; van Riemsdijk, W.H.; Koopal L.K. in *Metals Speciation, Separation and Recovery*, Patterson, J.W., Passino, R., Eds; Lewis Publishers: Michigan, USA, 1990; pp 330-353.

(22) Pagnanelli, F.; Petrangeli Papini, M.; Toro, L.; Trifoni, M.; Vegliò, F. *Environ. Sci. Technol*. **2000**, 34, 2773-2778.

(23) Gamble, D.S.; Undersdown, A.W.; Langford C.H. *Anal. Chem*. **1980**, 52, 1901-1908.

(24) Soldatov, V.S. *Ind. Eng. Chem. Res.* **1995**, 34, 2605-2611.

(25) Dupuy, N.; Douay, F. *Spectrochim. Acta, Part A* **2001**, 57, 1037-1047.

(26) Romero-González, M.E.; Williams, C.J.; Gardnier P.H.E. *Environ. Sci. Technol*. **2001**, 35, 3025-3030.

(27) Chapman, S.J.; Campbell, C.D.; Fraser, A.R.; Puri, G. *Soil Biol. Biochem.* **2001**, 33, 1193-1200.

(28) Hsu, J.H.; Lo, S.L. *Environ. Pollution* **1999**, 104, 189-196.

(29) Chen, J.P.; Lie, D., Wang, L.; Wu, S.; Zhang, B. *J. Chem. Technol. Biotechnol.* **2002**, 77, 657-662.

(30) Jeon, C.; Park, J.Y.; Yoo, Y.J. *Water Res*. **2002**, 36, 1814-1824.

(31) Rubinson, K.A.; Rubinson, J.F. *Análisis Instrumental*; Prentice Hall: Madrid, 2001.

(32) Huang, C.; Yang, Y.L. *Water Res*. **1995**, 29, 2455-2460.

(33) Puigdomènech, I. *Chemical Equilibrium Software Hydra and Medusa*, Inorganic Chemistry Department, Royal Institute of Technology, Stockholm, Sweden, www.inorg.kth.se/medusa (2001).

(34) Liem, D.H. *Acta Chem. Scand*. **1971**, 25, 1521-1534.